

Thermal Diffusivity Measurement for Multi-Layer Thin Films  
of Alternating Metallic Elements by Laser Produced Plasmas<sup>1</sup>

Yong W. Kim<sup>2, 3</sup>

- 
- 1 Paper presented at the Fourteenth Symposium on Thermophysical Properties  
June 25-30, 2000, Boulder Colorado, USA
  - 2 Department of Physics, Lewis Laboratory #16  
Lehigh University, Bethlehem, PA 18015-3182, USA.
  - 2 Author to whom correspondence should be addressed.

## ABSTRACT

The transport properties of condensed phase materials are in principle dependent on the local structure and composition of the specimen. This is particularly evident near the free surface of a solid alloy specimen where the morphology, composition and thermal diffusivity exhibit significant depth dependence, as demonstrated in our earlier study of depth-resolved thermal diffusivity of a galvanized steel specimen. A new non-contact method was used, based on time-resolved, spectroscopic measurement of the total mass removed from the specimen's surface representatively in elemental composition by a high-power laser pulse. We present a new study of a titanium thin film of varying thickness deposited on a copper substrate. The titanium thin film is first fabricated in a vacuum and then immediately analyzed for composition and thermophysical properties in situ, both by the method of representative laser-produced plasmas (LPP). Successive layers of the thin film, as exposed by LPP ablation, have revealed the dependence of the thermophysical properties on film thickness as well as depth. We have also observed the existence of a characteristic length over which the substrate influences the dynamics of thermal transport in the titanium thin film.

**KEY WORDS:** titanium thin films on copper substrate; thermal diffusivity of thin films; mass loss by laser-produced plasmas; non-contact measurement of thermal diffusivity; depth-dependent thermal diffusivity

## 1. INTRODUCTION

The transport properties of condensed phase materials are in principle dependent on the structure and composition of the specimen. This is particularly evident near the free surface of a solid alloy specimen where the morphology and composition exhibit significant depth dependence. This has been demonstrated in a depth-resolved measurement of the thermal diffusivity of a galvanized steel specimen by means of a new non-contact method based on time-resolved, spectroscopic measurement of the mass removed from the specimen's surface by a high-power laser pulse.[1,2]

The method is based on producing high-temperature, high-density plasma by means of a single high-power laser pulse incident on the specimen's surface. When the criterion that the receding free surface be kept in pace with the thermal diffusion front propagating into the bulk during laser heating is satisfied, the laser produced plasma (LPP) becomes representative of the specimen in its elemental composition.[3-6] The criterion for representative plasma production provides the measurement opportunity for thermal diffusivity because the mass entrained into the plasma plume is governed by the thermal diffusivity of the specimen. The total mass contained in the LPP plume, when measured, gives rise to a measure of the local thermal diffusivity.[7] We have further shown that the mass loss can be measured either by the impulse imparted on the target[8,9] or by time-resolved spectroscopy of the LPP plume[1,2].

The total mass from the surface results from a number of competing processes: surface heating; phase transitions leading to vapor production; dispersal of the plasma matters by diffusion

and hydrodynamic processes; and thermal diffusion into the bulk. These competing processes have been parameterized by three physical attributes of the constituent players in the form of a scaling relationship:[7]

$$\theta = C D_T^\alpha M^\beta H_f^\gamma . \quad (1)$$

Here  $\theta$  denotes the thickness in cm,  $D_T$  the thermal diffusivity in units of  $\text{cm}^2 \cdot \text{s}^{-1}$ ,  $M$  the molar weight, and  $H_f$  the heat of formation in  $\text{J} \cdot \text{g}^{-1}$ .  $C = 11.07 \pm 0.45$ ,  $\alpha = 0.91 \pm 0.01$ ,  $\beta = -\alpha$ , and  $\gamma = -1$ . In relating the thickness  $\theta$  of the ablated layer, it has been assumed that the condensed-phase layer has the mass density of the bulk. In cases where the surface layers exhibit a significant depth dependence, it is best represented in terms of mass loss,  $m_{\text{loss}}$ :  $m_{\text{loss}} = A \rho \theta$ , where  $\rho$  is the bulk mass density and  $A$  denotes the area of the LPP ablation crater.

In order to bring about a systematic analysis and modeling of the depth dependence, we have examined a system of a titanium thin film on a solid copper substrate. The specimens were fabricated by pulsed laser deposition of pure titanium. Depth-resolved measurements were then carried out for each specimen in situ.

## 2. EXPERIMENTAL SETUP FOR SPECIMEN FABRICATION AND ANALYSIS

The experimental setup is built around a small vacuum chamber consisting of a fused quartz cylinder. The specimen stage is implemented on a metal flange on one end, and a large-diameter fused quartz lens is mounted on the opposite end. The specimen stage consists of two mechanical feedthroughs, each a 6.36-mm cylindrical conductor, which can be translated along, and rotated about, its axis. The metal flange can be rotated about the chamber axis for the

purpose of aligning the specimen with respect to the laser beam and spectroscopic and imaging detectors outside. The vacuum chamber can be pumped down to  $10^{-6}$  Torr.

One of the feedthroughs is fitted with a multi-slot tray, one of which contains a pure titanium source specimen at  $45^\circ$  with respect to the laser beam axis. The second feedthrough is composed of two coaxial conducting cylinders, one inside the other. The smaller cylinder can be translated along, and rotated about, its axis. Together, they hold a hinged platform for the copper substrate and manipulate it from one orientation parallel to the laser beam during titanium deposition to another orientation that is perpendicular to the laser beam for subsequent LPP analysis. In this manner, fabrication and analysis of the titanium thin film specimens are carried out without exposing the specimens to the atmospheric air.

A Q-switched Nd:YAG laser provides the laser pulses at required pulsed power density in the range of  $10^9$  to  $10^{11}$  W/cm<sup>2</sup>. The laser beam and the detectors share the same lens mounted on the vacuum chamber by means of a dichroic mirror which reflects the laser pulse but transmits the LPP plume emissions over the entire near infrared to uv spectral range down to 200 nm.

The LPP plume is examined for elemental composition by means of time- and space-resolved spectroscopy. When such spectroscopic analyses are repeated, we obtain the depth profile of surface elemental composition. A spectrograph equipped with a gated, intensified CCD array detector is used for this purpose.

### 3. FABRICATION OF TITANIUM THIN FILM ON COPPER SUBSTRATE

Both the fabrication and analysis of titanium thin films are done by means of LPP plumes.

The experimental goals have been that a thin film specimen is first produced in the vacuum chamber and then the depth-resolved analysis and mass loss measurement of the specimen by spectroscopy is carried out immediately thereafter. To achieve these goals, the substrate must face the LPP plumes from the source during the deposition operation and then face the incident laser beam for LPP analysis and mass loss measurement. This two-step operation is accomplished by means of the hinged platform for the substrate described earlier.

The deposition rate of titanium on the substrate is first measured by ablating the titanium source at one laser power level for several hundred times. The mass change of the substrate is measured by weighing it with a digital microbalance. A deposition rate of  $(1.228 \pm 0.097) \times 10^{-6}$  g·cm<sup>-2</sup> per laser ablation has been established.

Three different thin film specimens have been fabricated by administering LPP plume depositions on copper substrates for an appropriate number of times to attain desired film thickness of  $1.25 \times 10^{-3}$ ,  $5.53 \times 10^{-4}$  and  $1.84 \times 10^{-4}$  g·cm<sup>-2</sup>, respectively. The spectroscopy of LPP plumes for depth-resolved mass loss determination was carried out immediately after each specimen had been fabricated.

#### 4. SPECTROSCOPIC MEASUREMENT OF MASS LOSS AND ITS CALIBRATION

Spectral emission intensities of a LPP plume in local thermodynamic equilibrium are linearly proportional to the elemental abundance within the detection volume of a wavelength-resolved intensity detection system, subject to the atomic transition probabilities of individual

spectral lines and the Maxwell-Boltzmann statistics of internal excitation within the plasma.[3] By choosing a group of emission lines, one can readily follow the relative changes in the mass entrained into the LPP plume from the specimen surface.

Fig. 1 shows a group of 59 spectra from the LPP plumes generated successively from a thin film of pure titanium on a solid copper substrate. The film thickness is  $1.25 \times 10^{-3} \text{ g}\cdot\text{cm}^{-2}$  as expressed in mass per unit area. There is the characteristic overshoot of the mass loss in the first few layers, followed by a plateau value that declines slowly over the twenty or so layers. A steep decline follows until the copper emission lines dominate.

Fig. 2 shows a group of 20 spectra from a second thin film specimen on the copper substrate. The film thickness is smaller and has an intermediate value of  $5.53 \times 10^{-4} \text{ g}\cdot\text{cm}^{-2}$ . The steep decline of the mass loss value sets in sooner at about the third layer. Fig. 3 shows the spectra for a third thin film at  $1.84 \times 10^{-4} \text{ g}\cdot\text{cm}^{-2}$  in thickness. Only the first layer shows any significant mass loss, and the characteristic decline is compressed into the small span of five LPP ablations.

The emission spectra of LPP plumes from a solid target of pure titanium show rather different development as the surface layers are examined one after another. This is shown in Fig. 4. There is the overshoot of mass loss at the first few surface layers, followed by a slight decline to a steady state response.

A comparison of the four sets of the LPP plume spectra shows the general pattern of the near-surface thermophysical properties. The mass loss per LPP ablation, as derived from LPP plume emission spectra, are summarized in Fig. 5 for the four cases shown in Figs. 1 through 4.

Firstly, the mass loss overshoot seems to be due to loose packing of titanium atoms to levels below that of the bulk mass density. This would increase the surface emissivity and absorption coefficient as well as increase the thermal diffusivity. Both of these effects contribute to an increase of the mass loss, as we have observed. The relative importance of these two effects can be delineated in principle by measuring the surface reflection coefficient, but we have not carried out the measurement to date.

Secondly, in the case of the thickest thin film of Fig. 1, the mass loss approaches that of bulk titanium, shown in Fig. 4, over the next 20 to 25 layers. This means that the influence of the copper substrate as an efficient thermal reservoir at room temperature has not materialized within the laser pulse duration. With the intermediate and thinnest films of Fig. 2 and Fig. 3, the spans of depth over which the mass loss approaches that of the bulk are severely truncated. It means that the influence of the copper substrate on thermal transport within the thin film of titanium extends over the next 35 LPP ablation layers, and this translates to about  $4 \times 10^{-4} \text{ g} \cdot \text{cm}^{-2}$  in thickness.

Thirdly, the large mass loss from the thinnest film points to the fact that the compactness of the thin film is primarily governed by the thickness of the titanium thin film, i.e., the total number of titanium atoms, and to a lesser extent by the copper atoms in the substrate. Finally, we have not assigned definitive values for the thickness of the successive LPP ablation layers due to the fact that the mass density profile of these near-surface layers is unknown at this time. Some estimates can be made, however, on the basis of the measurement with the solid specimen of pure titanium shown in Fig. 4. The mass loss from the deep lying layers of the solid specimen is  $0.2 \text{ } \mu\text{g}$  per LPP ablation. This gives 6.3 nm for the thickness of the inner layers using the bulk mass density



of  $4.50 \text{ g}\cdot\text{cm}^{-3}$ , [10] which is justified by the fact that the bulk response has been demonstrated at such depths. The mass loss overshoot at the outermost layers of the titanium thin films suggests that the local mass density may be lower than that of the bulk by as much as a factor of two or three. This puts the thickness of the outer ablation layers varying between 13 and 20 nm.

Determination of the absolute mass loss is achieved by calibration. A preset number of LPP ablations in the range between 100 and 500 are carried out on a solid titanium specimen and its accumulated mass loss is measured by means of a digital microbalance. This gives the average mass loss per LPP ablation of  $0.20 \text{ }\mu\text{g}$ . The emission spectrum is also taken from every tenth or twentieth LPP plume. The integrated intensity of a set of selected titanium emission lines is then calibrated as the total mass of the titanium atoms and ions in the LPP plume by relating it to the measured mass loss. Once the calibration has been carried out, the total mass of the surface layer removed by each LPP ablation is determined entirely by spectroscopy without contact with the specimen.

## 5. ROLE OF SUBSTRATE IN THERMAL DIFFUSION IN THIN FILMS

The interesting question has to do with the rather large distance over which the copper substrate affects the mass loss of the titanium thin film. Given that the laser pulse drives the surface temperature high, sufficient to sustain the mass loss rate, the reduction in the mass loss must mean that the copper substrate is lowering the temperature of the leading edge of the thermal diffusion front. This can be readily demonstrated by examining the effect of the substrate on the steady-state temperature profile for a two-slab geometry. Let us consider a thin film of thickness

$L_{tf}$  and thermal conductivity  $K_{tf}$  in contact with a substrate of thickness  $L_s$  and thermal conductivity  $K_s$ . We assign the surface temperature of the thin film to be higher at  $T_h$  than  $T_i$ , the base temperature of the substrate, as is the case for LPP ablation. Defining the fractional thickness of the thin film by  $\alpha = L_{tf} / (L_{tf} + L_s)$  and thermal conductivity ration by  $\beta = K_{tf} / K_s$ , the temperature at the interface,  $T_i(\beta)$ , can be found:

$$T_i(\beta) = [\beta (1-\alpha) T_h + \alpha T_i] / [\alpha + \beta (1-\alpha)] . \quad (2)$$

This interface temperature can be compared with that at the same position inside a single slab of combined thickness  $L_{tf}+L_s$  and uniform thermal conductivity (i.e.,  $\beta=1$ ). The temperature ratio,  $T_i(\beta) / T_i(1)$ , is plotted in Fig. 6 as a function of  $\beta$  for  $T_h = 4000$  K and  $T_i = 300$  K. It is clear that for  $\beta < 1$  the interface temperature is suppressed by the substrate for all values of  $\alpha$ . This has the effect of lowering the thermal diffusion velocity, which in turn reduces the mass loss by LPP ablation. For the present titanium-copper system,  $\beta = 0.055$ . [10]

## 7. CONCLUSIONS

We have investigated the mass loss by LPP ablation as a measure of the local thermal diffusivity for thin films of titanium on a copper substrate. The response of the titanium-copper system has been examined as a function of titanium thin film thickness. Both the fabrication of the thin film and its surface analysis were carried out in situ, one immediately following the other without exposure to the atmospheric air. The desired film thickness was obtained by repetitively

depositing the titanium atoms in the LPP plumes from a pure titanium source. The thickness of the titanium film deposited per LPP ablation was independently determined in advance.

Analysis of the response of the thin film in the form of mass loss shows that the mass density of the titanium in the thin film depends on both the film thickness and the depth from the outermost surface. This tendency affects the spectral reflection coefficient[11] and the heat of formation as well as the thermal diffusivity, thus bringing about the depth dependence of the LPP mass loss.

We have found that the film thickness is manifested in the dynamics of LPP mass loss in yet another way for the system of a thin film built on a substrate of higher thermal conductivity. The substrate lowers the temperature of the interface from that of a single-element medium. The lowering in turn thins the surface layer of the thin film, which can be heated to melting and evaporation within the duration of the laser pulse. The distance over which the substrate has a cooling effect can be a significant part of the thin film and is most likely dependent on the ratio of the thermal conductivity of the two materials.

The above summary seems quite reasonable on a physical ground. Additional measurements of the surface properties, as the new layers are exposed in successive LPP ablations, will help strengthen the understanding of the thermal transport properties of multi-layered structures. It is possible to determine the reflection coefficient of the surface within the framework of the present in-situ experiment, and we intend to incorporate this measurement prior to spectroscopic measurement of each LPP plume toward this end.

## REFERENCES

1. Y.W. Kim, *Int. J. Thermophys.* **20**: 1315 (1999).
2. Y.W. Kim, in *Thermal Conductivity 25/Thermal Expansion 13*, C. Uher and D. Morelli, eds. (Technomic Publishing, Lancaster, PA, 2000). p. 15.
3. Y.W. Kim, in *Laser-Induced Plasmas and Applications*, L.J. Radziemski and D.A. Cremers, eds., (Marcell Dekker, New York, 1989). Chapter 8.
4. Y.W. Kim, *High Temp. Sci.* **26**: 57 (1990).
5. Y.W. Kim, in *Intelligent Processing of Materials*, H.G.N. Wadley and W.E. Eckhart, eds., (The Minerals, Metals and Materials Society, Warrendale, PA, 1990). p. 317.
6. Y.W. Kim, in *Advanced Sensing, Modeling, and Control of Materials Processing*, E.F. Mattys and B. Kushner, eds., (TMS, Warrendale, PA, 1992). p.44.
7. Y.W. Kim, *Int. J. Thermophys.* **14**: 397 (1993).
8. Y.W. Kim and C.S. Park, *Int. J. Thermophys.* **17**: 713 (1996).
9. Y.W. Kim, and C.S. Park., *Int. J. Thermophys.* **17**: 1125 (1996).
10. D.E. Gray, ed., *AIP Handbook, Third Edition*, (McGraw-Hill, NY, 1972).
12. W.M. Rohsenow, J.P. Hartnett and Y.I. Cho, *Handbook of Heat Transfer*, 3<sup>rd</sup> Edition (McGraw-Hill, NY, 1998). Chapter 16.

## FIGURE CAPTIONS

Figure 1. Emission spectra of LPP plumes, taken successively from a titanium film of thickness  $1.25 \times 10^{-3} \text{ g} \cdot \text{cm}^{-2}$ , given in mass per unit area, deposited on a solid copper substrate. The wavelength range is from 367.1 nm (detector pixel 300) to 608.4 nm (detector pixel 1000).

Figure 2. Emission spectra of LPP plumes, taken successively from a titanium film of thickness  $5.53 \times 10^{-4} \text{ g} \cdot \text{cm}^{-2}$ , given in mass per unit area, deposited on a solid copper substrate. The wavelength range is from 367.1 nm (detector pixel 300) to 608.4 nm (detector pixel 1000).

Figure 3. Emission spectra of LPP plumes, taken successively from a titanium film of thickness  $1.84 \times 10^{-4} \text{ g} \cdot \text{cm}^{-2}$ , given in mass per unit area, deposited on a solid copper substrate. The wavelength range is from 367.1 nm (detector pixel 300) to 608.4 nm (detector pixel 1000).

Figure 4. Emission spectra of LPP plumes, taken successively from a solid specimen of pure titanium. The wavelength range is from 367.1 nm (detector pixel 300) to 608.4 nm (detector pixel 1000).

Figure 5. Mass loss per LPP ablation as function of the number of successive LPP ablations is shown for the four different specimens in Figs.1 through 4: (a) titanium film of thickness  $1.84 \times 10^{-4} \text{ g} \cdot \text{cm}^{-2}$ , deposited on a solid copper substrate; (b) titanium film of thickness  $5.53 \times 10^{-4} \text{ g} \cdot \text{cm}^{-2}$ ; (c)

titanium film of thickness  $1.25 \times 10^{-3} \text{ g} \cdot \text{cm}^{-2}$ ; and (d) pure solid titanium specimen. The solid curves show the cumulative mass losses for the respective specimens in relative scale. The short solid line in Fig. 5d on the right hand side indicates the calibration by a digital microbalance for mass loss at  $0.2 \text{ } \mu\text{g}$ .

Figure 6. Calculated steady-state temperature at the interface between a thin film and a substrate, relative to the temperature within the substrate medium without the thin film, as function of the ratio  $\beta$  of the thin-film's thermal conductivity to that of the substrate. Three different values of the fractional thickness  $\alpha$  of the thin film are used.

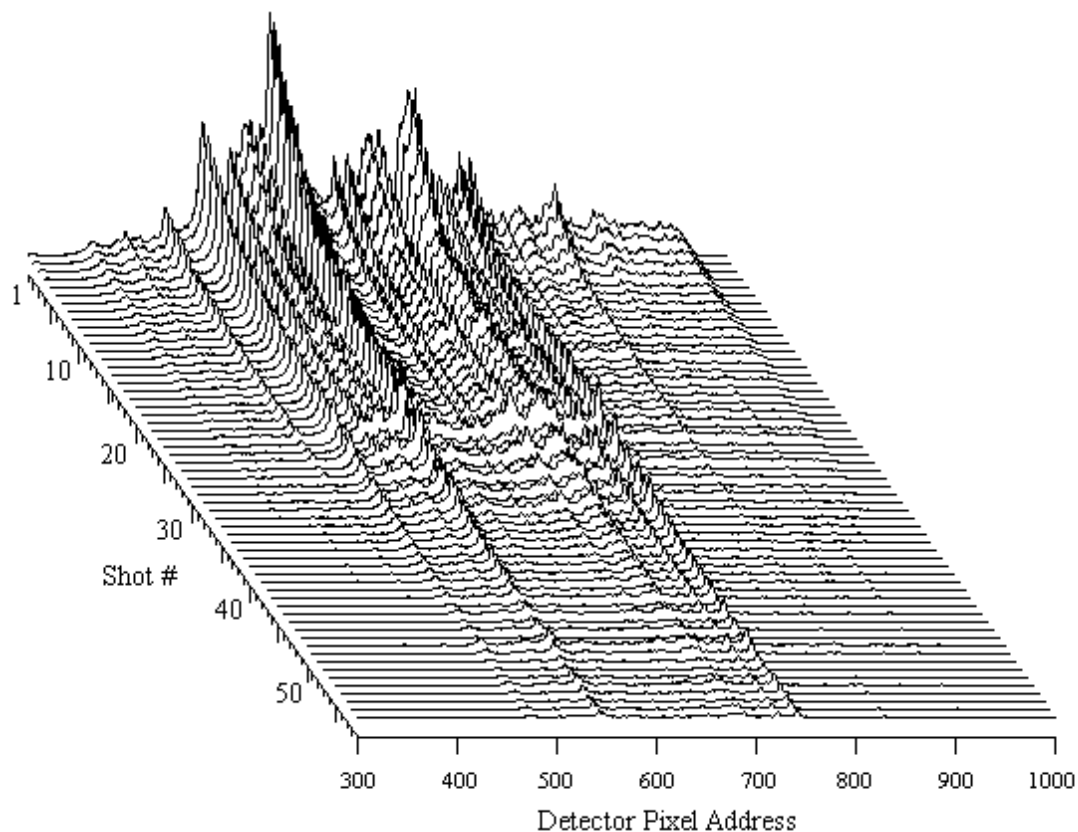


Figure 1. Emission spectra of LPP plumes, taken successively from a titanium film of thickness  $1.25 \times 10^{-3} \text{ g} \cdot \text{cm}^{-2}$ , given in mass per unit area, deposited on a solid copper substrate. The wavelength range is from 367.1 nm (detector pixel 300) to 608.4 nm (detector pixel 1000).

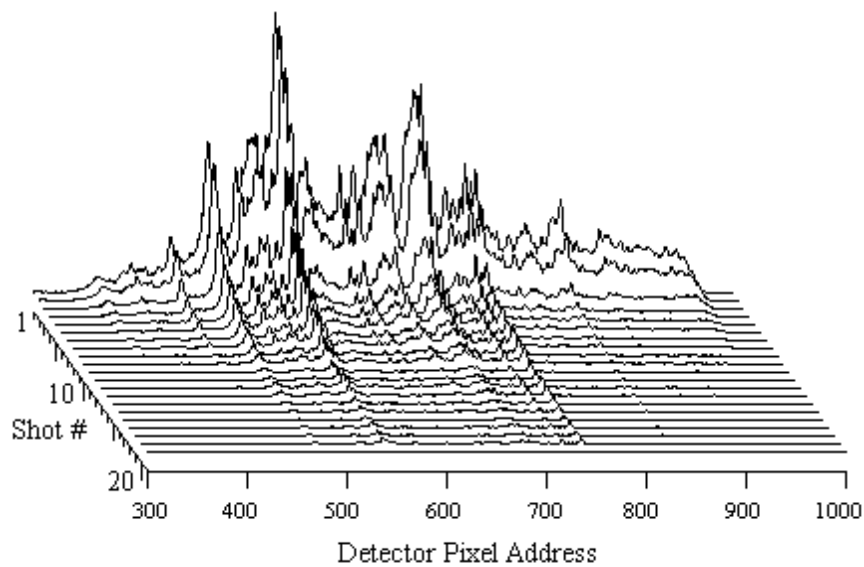


Figure 2. Emission spectra of LPP plumes, taken successively from a titanium film of thickness  $5.53 \times 10^{-4} \text{ g} \cdot \text{cm}^{-2}$ , given in mass per unit area, deposited on a solid copper substrate. The wavelength range is from 367.1 nm (detector pixel 300) to 608.4 nm (detector pixel 1000).



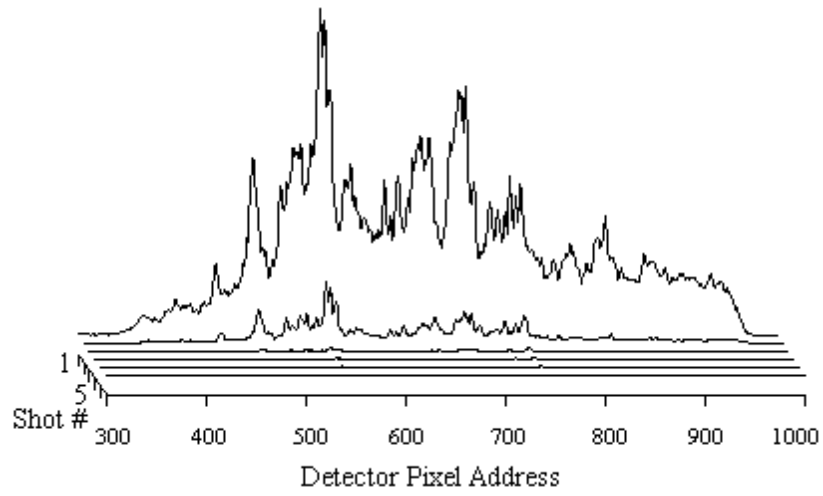


Figure 3. Emission spectra of LPP plumes, taken successively from a titanium film of thickness  $1.84 \times 10^{-4} \text{ g} \cdot \text{cm}^{-2}$ , given in mass per unit area, deposited on a solid copper substrate. The wavelength range is from 367.1 nm (detector pixel 300) to 608.4 nm (detector pixel 1000).

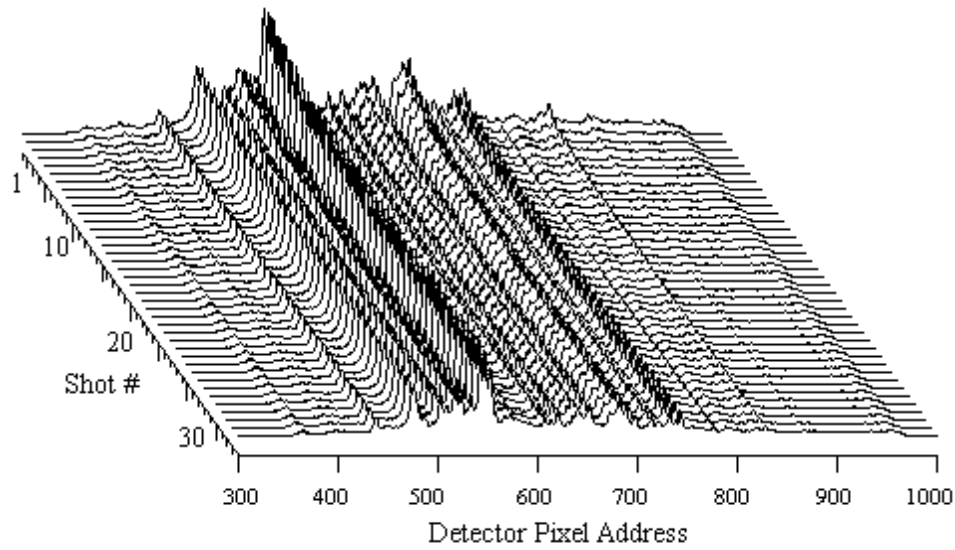


Figure 4. Emission spectra of LPP plumes, taken successively from a solid specimen of pure titanium. The wavelength range is from 367.1 nm (detector pixel 300) to 608.4 nm (detector pixel 1000).

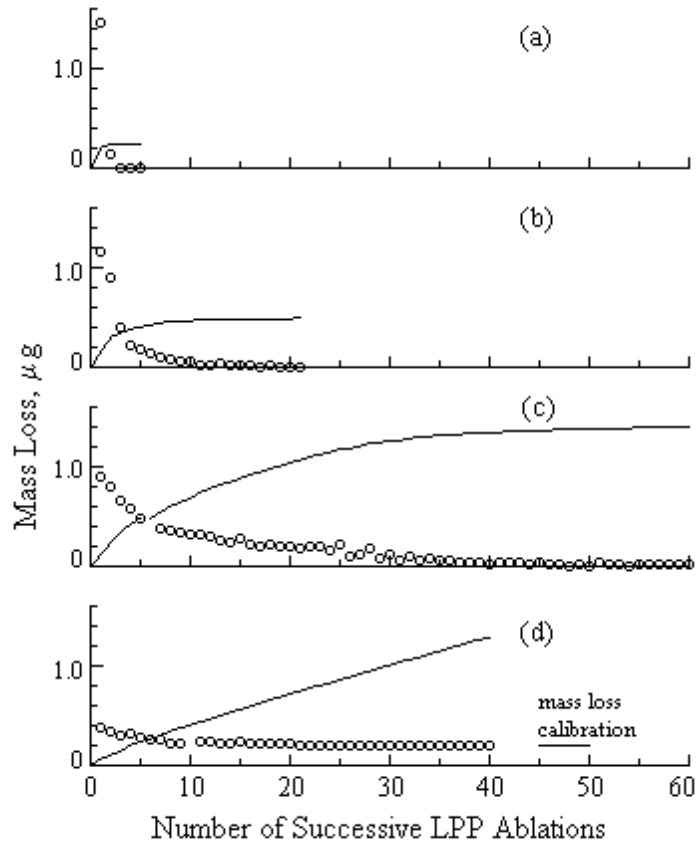


Figure 5. Mass loss per LPP ablation as function of the number of successive LPP ablations is shown for the four different specimens in Figs.1 through 4: (a) titanium film of thickness  $1.84 \times 10^{-4} \text{ g}\cdot\text{cm}^{-2}$ , deposited on a solid copper substrate; (b) titanium film of thickness  $5.53 \times 10^{-4} \text{ g}\cdot\text{cm}^{-2}$ ; (c) titanium film of thickness  $1.25 \times 10^{-3} \text{ g}\cdot\text{cm}^{-2}$ ; and (d) pure solid titanium specimen. The solid curves show the cumulative mass losses for the respective specimens in relative scale. The short solid line in Fig. 5d on the right hand side indicates the calibration by a digital microbalance for mass loss at  $0.2 \mu\text{g}$ .

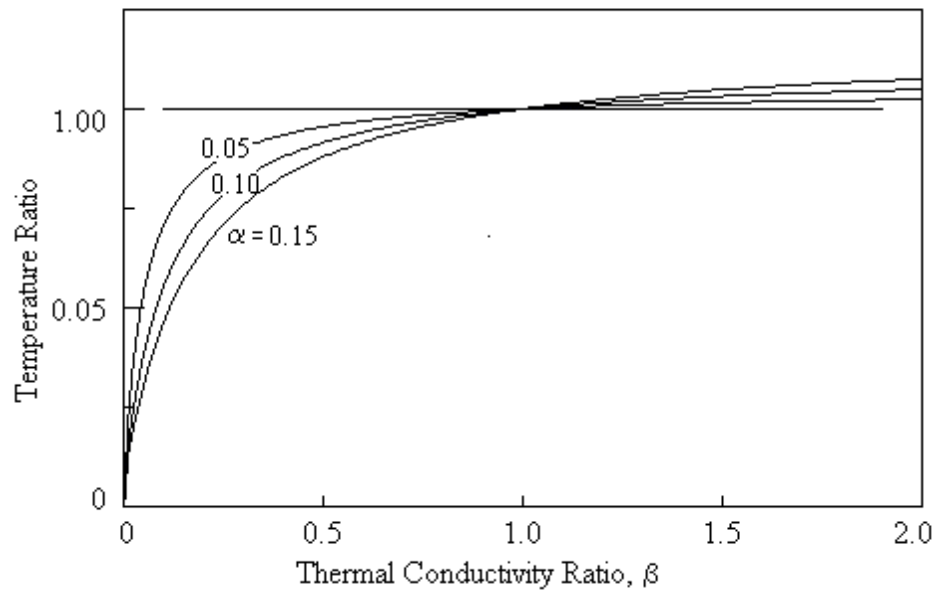


Figure 6. Calculated steady-state temperature at the interface between a thin film and a substrate, relative to the temperature within the substrate medium without the thin film, as function of the ratio  $\beta$  of the thin-film's thermal conductivity to that of the substrate. Three different values of the fractional thickness  $\alpha$  of the thin film are used.